1982ApJ...256..139M

THE ASTROPHYSICAL JOURNAL, 256:139–150, 1982 May 1
© 1982. The American Astronomical Society. All rights reserved. Printed in U.S.A.

THE MOLECULAR CLOUD COMPLEX IN THE VICINITY OF IC 5146

W. H. MCCUTCHEON
Department of Physics, University of British Columbia
R. S. ROGER
Dominion Radio Astrophysical Observatory, Herzberg Institute of Astrophysics
AND
R. L. DICKMAN[1]
The Aerospace Corporation, Los Angeles, California
Received 1981 April 3; accepted 1981 November 6

ABSTRACT

CO observations of the molecular cloud complex in the vicinity of IC 5146 reveal three regions of enhanced emission, all lying around the periphery of the Sharpless region S125. The most intense region has a peak CO line temperature of 41 K. The continued existence of this hot spot can be accounted for by an embedded protostar of luminosity class between B0.5 and B1. A comparison with H I observations of about the same spatial and velocity resolution shows that the surrounding H I cloud emission is generally strong where the CO emission is weak.

The velocity of the H II region, S125, is blueshifted with respect to the gas behind it by 5.6 km s^{-1}. This has yielded an estimate for the expansion age of the H II region of about 10^5 yr, a factor of 30 smaller than the age given for the stellar cluster.

The whole complex along the elongated dust lane, to a distance of 16.1 pc from the center of S125, shows a velocity gradient of 0.26 km s^{-1} pc^{-1}. Rotation is considered as a possible cause for the extended geometry of the region.

Subject headings: interstellar: molecules— nebulae: H II regions — nebulae: individual

I. INTRODUCTION

IC 5146 is a stellar cluster in the direction of Cygnus. The name has also been applied to the Sharpless region S125, a small-diameter H II region in the cluster powered by the single B0 V star BD +46°3474. The H II region lies on the near side of a large dark cloud from which in turn a long, narrow complex of dark clouds extends to the west (see Fig. 1).

The association of the dark cloud complex and the H II region was indicated by the H I measurements of Riegel (1967) and was more recently firmly established by CO observations (Lada and Elmegreen 1979; Israel 1980) and by the high-resolution H I synthesis observations reported in the companion paper of Roger and Irwin (1982). These latter results reveal a large H I cloud located mainly behind the H II region and coincident with the "bulb" of extinction.

In recent years there has been considerable interest in molecular clouds associated with Sharpless regions and in the interaction between the two (Evans, Blair, and Beckwith 1977; Blair *et al.* 1978). CO observations have proven to be very fruitful in delineating the overall structure of these regions. The presence of the H I cloud and the relatively simple geometry of the H II region and its immediate environment stimulated our interest in IC 5146, and we undertook a 2.6 mm CO study to further clarify the relationship among the ionized, atomic, and molecular gas regions. Such observations can lead to a better understanding of the processes involved in star formation.

CO observations in the vicinity of IC 5146 have previously been reported by Milman *et al.* (1975), Israel (1978, 1980), Lada and Elmegreen (1979), and McCutcheon *et al.* (1980). Lada and Elmegreen made the most detailed observations, with their ^{12}CO results showing three regions of enhanced emission around S125; however, they obtained ^{13}CO results at only 20 selected positions.

In this paper we present results from a much more fully sampled survey of ^{12}CO and ^{13}CO, with observations around S125 spaced at one beamwidth intervals (in some directions at half-beamwidth intervals) and extended to the edge of the extinction where ^{13}CO line intensities fall below the noise. We have also observed ^{12}CO or ^{13}CO at eight positions over a span of 1° along the dark lane extending to the northwest. $C^{18}O$ was observed at six selected positions. These profiles were used to derive isotope ratios which were reported in an earlier paper (McCutcheon *et al.* 1980).

In § II we discuss the observations and data analysis, and in § III we present the results of the CO maps and discuss the cloud structure. Section IV contains a discussion of the velocity structure of the cloud complex. Comparison is also made with the H I maps of Roger

[1] Now at Five College Radio Astronomy Observatory, University of Massachusetts, Amherst, Massachusetts.

© American Astronomical Society • Provided by the NASA Astrophysics Data System

1982ApJ...256..139M

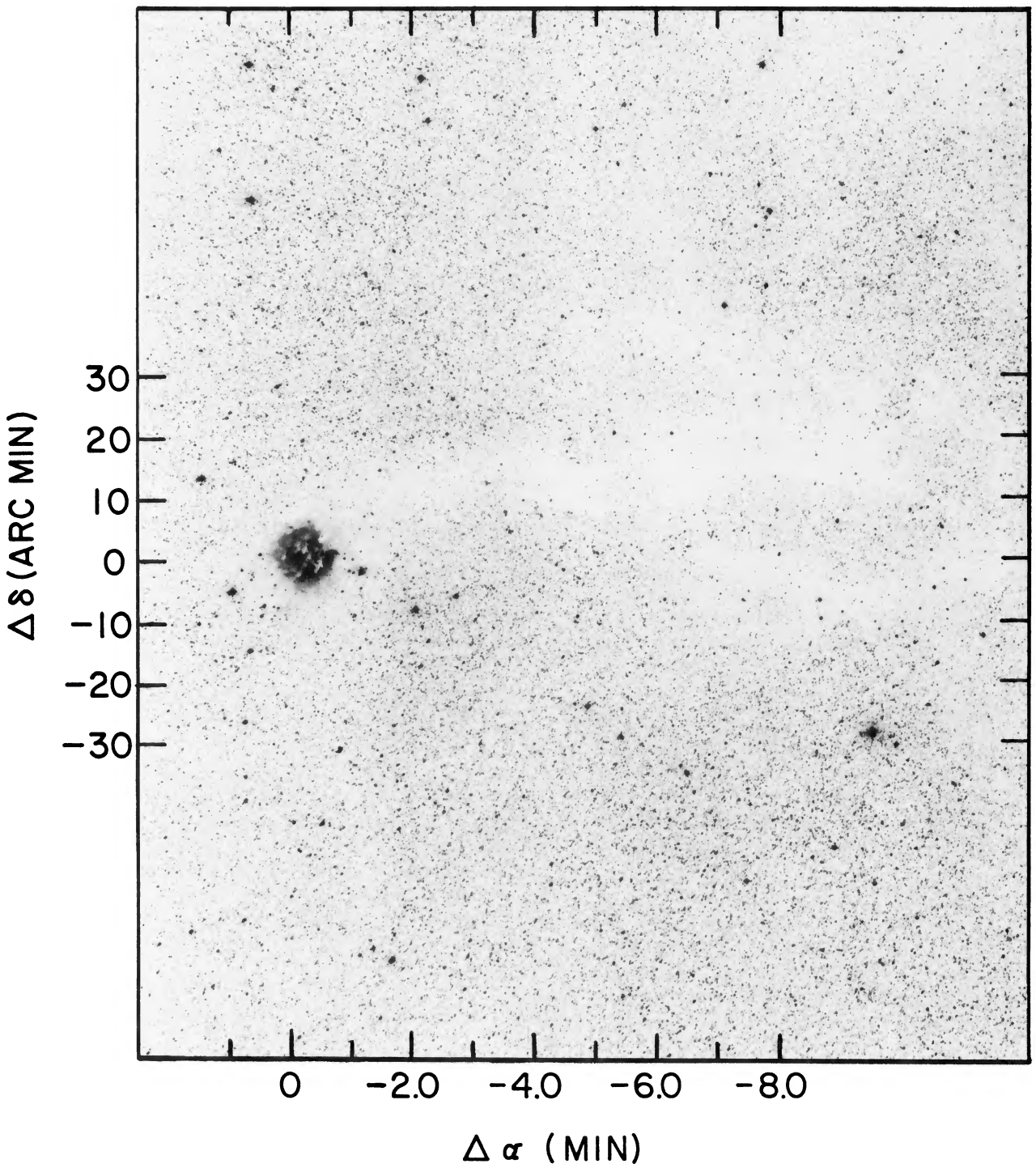

FIG. 1.—The dark cloud complex in the vicinity of IC 5146 and the H II region S125 reproduced from the Palomar Sky Survey blue print. The center coordinate is $\alpha(1950) = 21^h51^m37^s$, $\delta(1950) = 47°02'07''$.

© American Astronomical Society • Provided by the NASA Astrophysics Data System

1982ApJ...256..139M

and Irwin (1982) which were obtained with almost the same spatial and velocity resolutions used in this work.

II. OBSERVATIONS AND DATA ANALYSIS

Most of the data were taken in 1977 November and December using the 4.6 m telescope at the Aerospace Corporation.[2] Equipment parameters and details relating to calibration procedures are given in McCutcheon *et al.* (1980). The system temperature for the observations of both isotopes was approximately 1500 K single-sideband.

A few additional ^{12}CO observations were made at positions along the elongated dust lane in 1979 June using the 4.6 m radio telescope at the University of British Columbia. The spatial and velocity resolutions were the same as for the Aerospace observations, and the system temperature was 1000 K single-sideband. Data were obtained in a frequency switching mode, and the calibration procedure was similar to that described for the Aerospace data.

To reduce the carbon monoxide data, the optical depth $\tau(^{13}\mathrm{CO})$ was determined at each velocity in the line assuming LTE, i.e., the excitation temperature of ^{13}CO is constant along the line of sight and equal to that inferred from the optically thick ^{12}CO line. The column density of ^{13}CO was then calculated from the quantity $\int \tau dv$ and the partition function, which was evaluated to $J = 10$ assuming a constant rotational temperature equal to the excitation temperature.

A search was also made in 1978 May for H_2O emission using the 43 m telescope of NRAO[3] and the new low-noise maser. The system temperature (including sky contribution) was about 90 K, and the velocity resolution was 0.18 km s^{-1}. No H_2O emission was detected (see § III).

III. STRUCTURE IN THE VICINITY OF S125

a) The Three Concentrations

Figures 2 and 3 show ^{12}CO and ^{13}CO contours, integrated over all velocities, superposed on enlargements of the Palomar Sky Survey blue print for the IC 5146 region. Figure 2 also shows two H I contours integrated over the same velocity range. The most striking feature is the existence of three regions of enhanced emission, all lying around the edge of the H II region. These three hot spots, lying to the east (the brightest or most intense), the north, and the west, will be denoted HS1, HS2, and HS3, respectively. In contrast, the emission from the center of the H II region is somewhat depressed, with the ^{13}CO column density being a factor of 2 lower than the average value obtained in the cold material in the dark lane away from the H II region.

Figures 4 and 5 show contour plots of T_{12}* and T_{13}*, respectively, for different velocities, placed on the same photograph shown in Figures 2 and 3. The three hot spots peak at distinctly different velocities; a point which will be discussed further in the next section. Table 1 lists the coordinates and velocities of all the peaks detected in the three hot spots. Some peaks, e.g., 2 and 5 in Table 1, are only clearly seen on contour plots at a specific velocity. The peaks which are most prominent in the three hot spots of Figures 2 and 3 are 1, 3, 4, 6, and 8.

Masses for regions where the excitation temperature is fairly constant were determined by summing the column densities within the outermost contours of each of the three hot spots and multiplying by the surface area contained within the beam. Values of molecular hydrogen column density were obtained using the relation from Dickman (1978), and we used a value for the mean molecular weight $\mu = 2.33$ which is appropriate for a mixture of H_2 and He (Field 1973). For the hot spots, where the excitation temperature is not constant along the line of sight, the evaluation of each column density involves two integrals, $\int \tau dv$, mentioned in § II, and the integral of the excitation temperature along the line of sight, $\int T_x dl$. To determine the column density, we assumed a simple velocity law (e.g., Dickman, McCutcheon, and Shuter 1979) and associated each data point in a spectral line with a particular location in a cloud, thus obtaining T_x. (Fig. 6 shows T_x plotted as a function of radial distance for HS1.) We evaluated several column densities in this manner and found, surprisingly, that the values differed by at most 15% from the values obtained assuming a constant T_x along the line of sight.

TABLE 1

^{12}CO AND ^{13}CO PEAKS FROM THE CONTOUR PLOTS

(The central coordinate is: $\alpha(1950) = 21^h51^m37^s$, $\delta(1950) = 47°02'07''$)

Peak	$\Delta\alpha$ (s)	$\Delta\delta$ (arcmin)	V_{LSR} (km s^{-1})	T_{12}*(K)	T_{13}*(K)		Mass ($M_\odot$)
1[a,b]	22.0	−3.67	7.55	41	8	HS1	247
2[c]	44.0	−4.82	6.25	13	5		
3[a]	15.0	4.93	8.20	25	7	HS2	95
4[a,d]	15.0	2.58	8.20	25	...		
5[e]	0.4	4.85	7.55	17	...		
6[a]	−29.0	−2.38	5.60	19	4	HS3	88
7[f]	−44.0	0.0	6.25	17	...		
8[a,g]	−44.0	−2.47	6.90	...	4		
9[g]	−59.0	0.0	6.90	...	3		

[a] The major peaks seen in HS1, HS2, and HS3 in Figures 1 and 2.

[b] This peak is ~3′ from an infrared source with K magnitude between +7 and +8 found by Elias 1978. However, it is suspected to be a background source.

[c] Most clearly seen on the ^{12}CO contour plot at $V_{LSR} = +6.25$ km s^{-1}; only an extension on the integrated contours.

[d] Only an extension on the ^{13}CO integrated contours.

[e] Visible on the ^{12}CO contour plot at $V_{LSR} = +7.55$ km s^{-1}. Coincident with a source having $S_{1415} = 62$ mJy (Israel 1977; Roger and Irwin 1982) which is suspected to be a background source.

[f] Visible only on ^{12}CO contours.

[g] Visible only on ^{13}CO contours.

[2] The Aerospace Spectral-Line Radio Program was supported jointly by the National Science Foundation grant MPS 73-04554 and the Aerospace Corporate Programs for Research and Investigation.

[3] The National Radio Astronomy Observatory is operated by Associated Universities, Inc., under contract with the National Science Foundation.

© American Astronomical Society • Provided by the NASA Astrophysics Data System

1982ApJ...256..139M

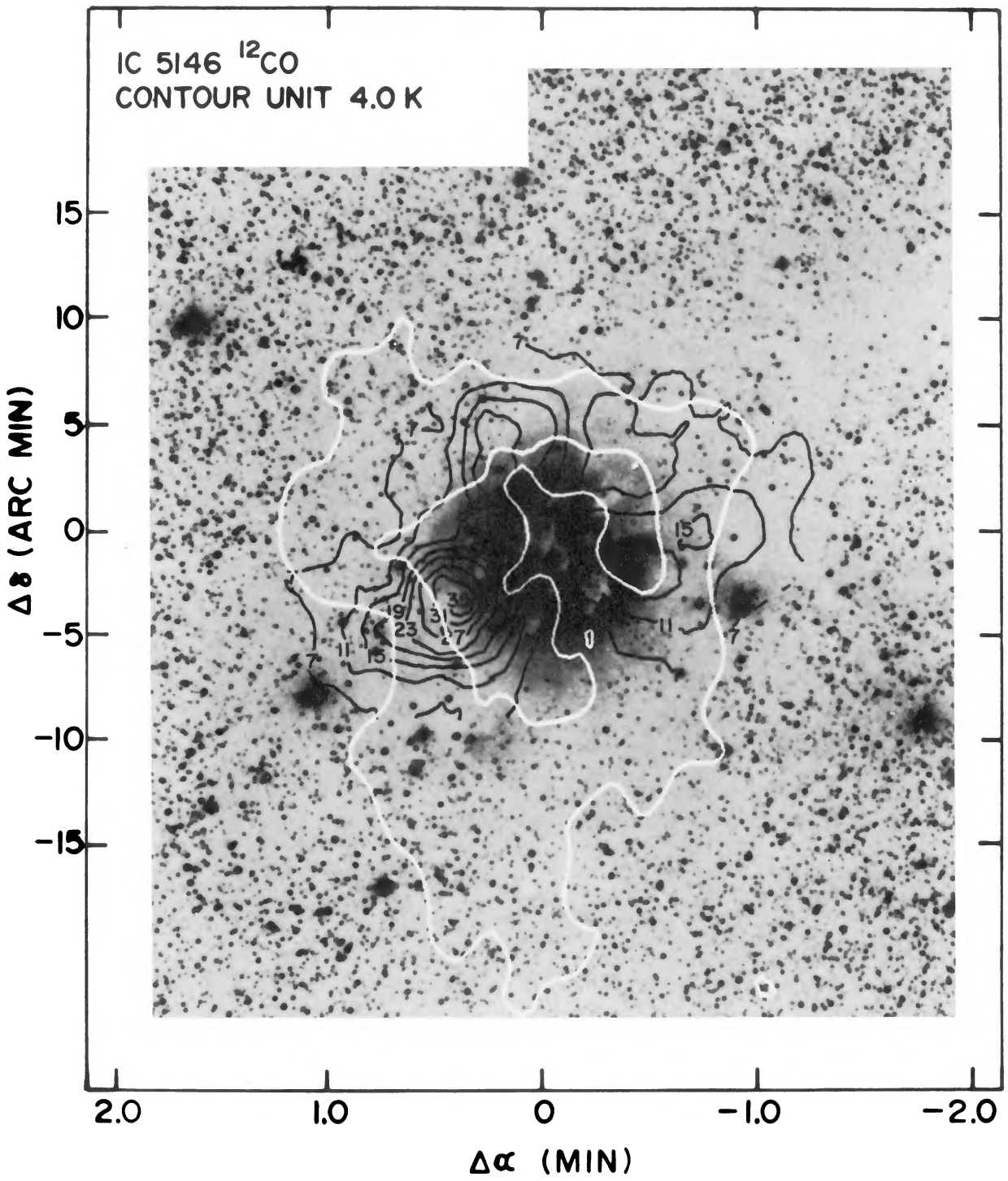

FIG. 2.—Black lines are ^{12}CO contours integrated over the velocity range 5.60–8.85 km s^{-1}. White lines are H I contours from Roger and Irwin (1982) integrated over the velocity range 5.5–9.0 km s^{-1}. The two H I contours represent 4.50×10^{20} (*inner contour*) and 2.25×10^{20} atoms cm^{-2} (*outer contour*). Photograph is reproduced from the Palomar Sky Survey prints. Center coordinate is the same as in Fig. 1.

© American Astronomical Society • Provided by the NASA Astrophysics Data System

1982ApJ...256..139M

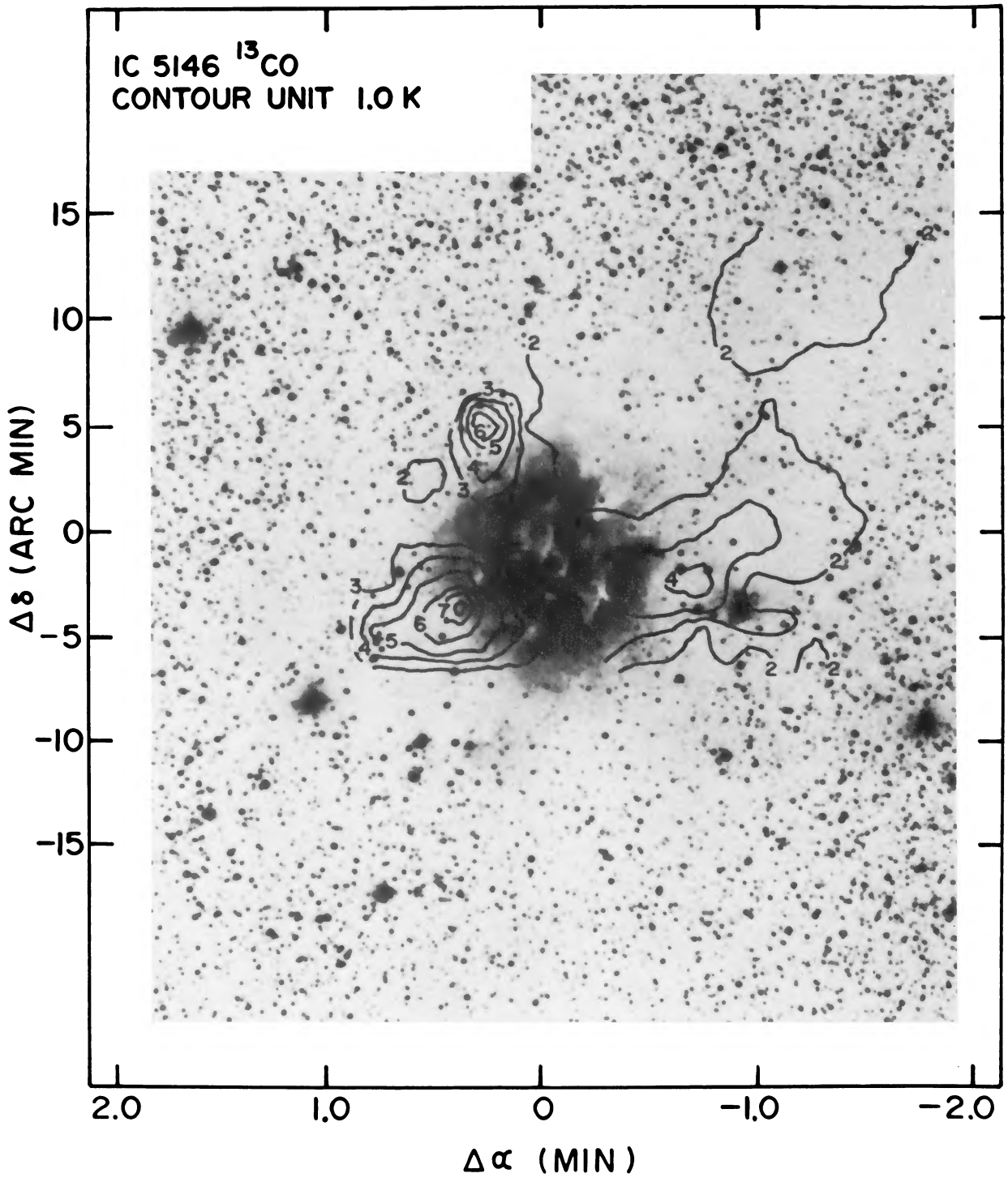

FIG. 3.—^{13}CO contours integrated over the velocity range 6.25–8.85 km s^{-1} placed on a photograph reproduced from the Palomar Sky Survey prints. Center coordinate is the same as in Fig. 1.

© American Astronomical Society • Provided by the NASA Astrophysics Data System

1982ApJ...256..139M

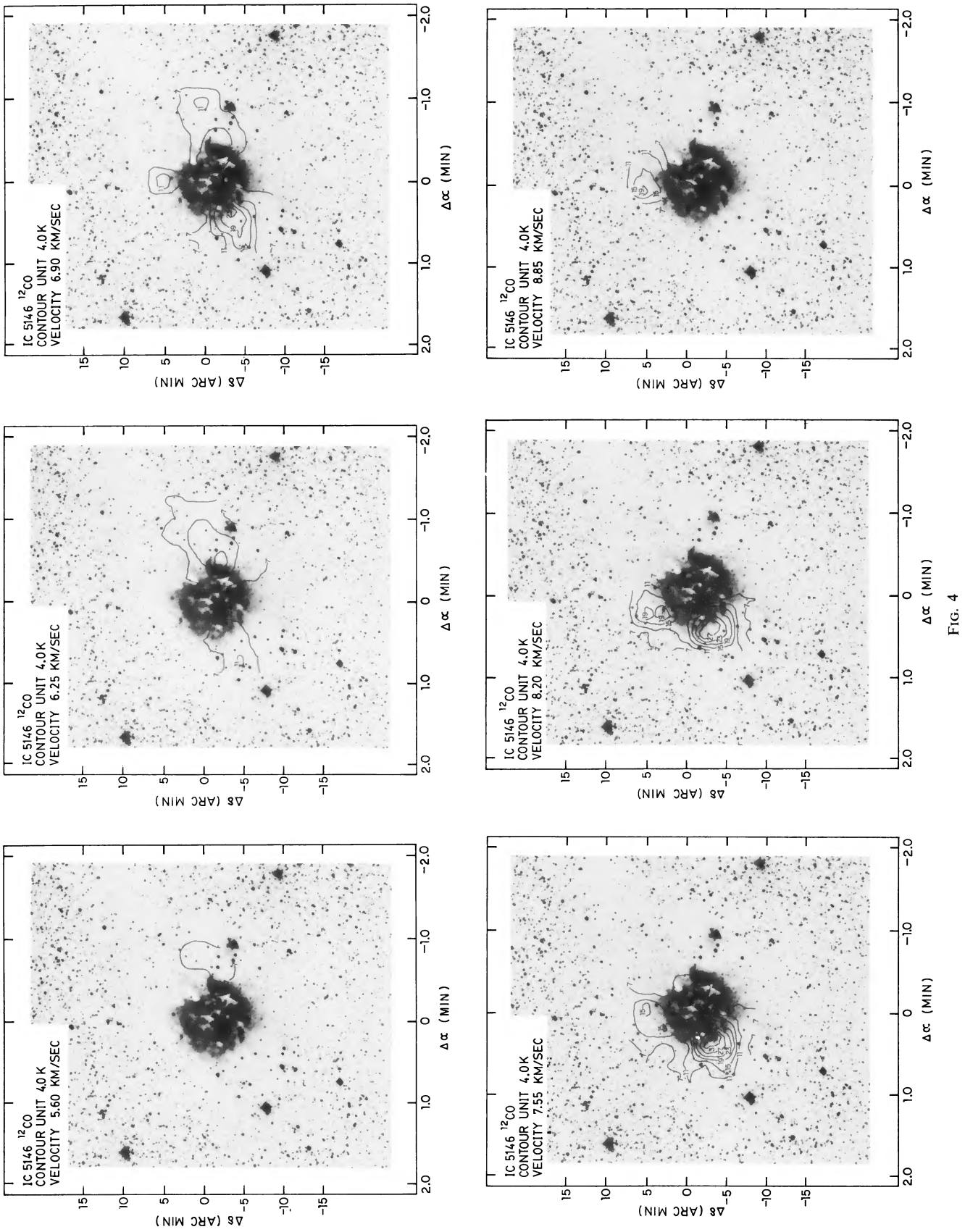

FIG. 4

© American Astronomical Society • Provided by the NASA Astrophysics Data System

1982ApJ...256..139M

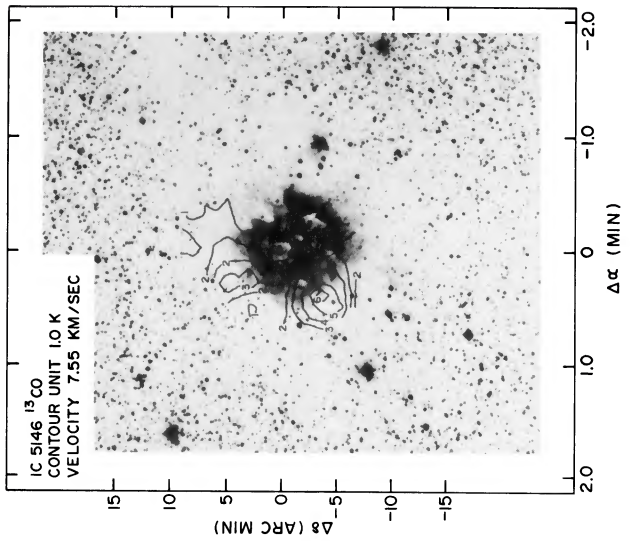

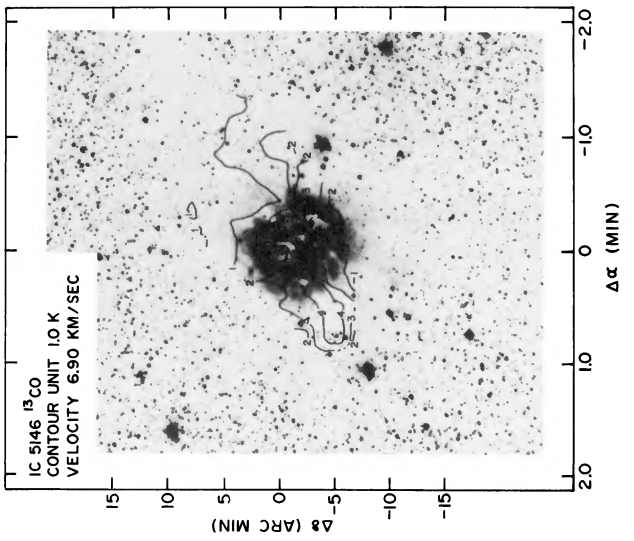

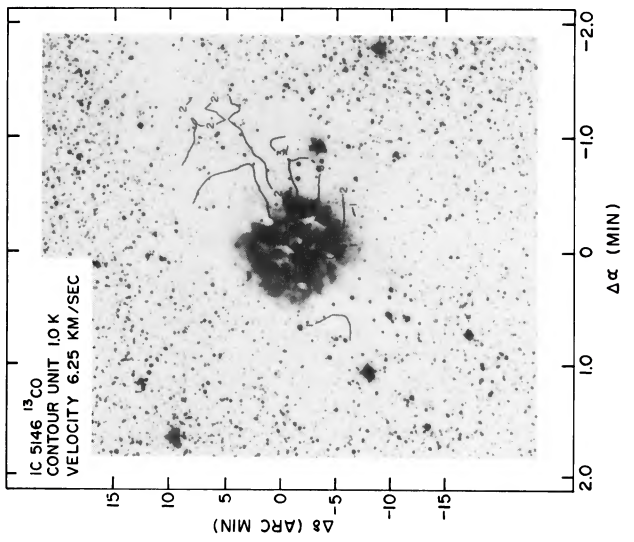

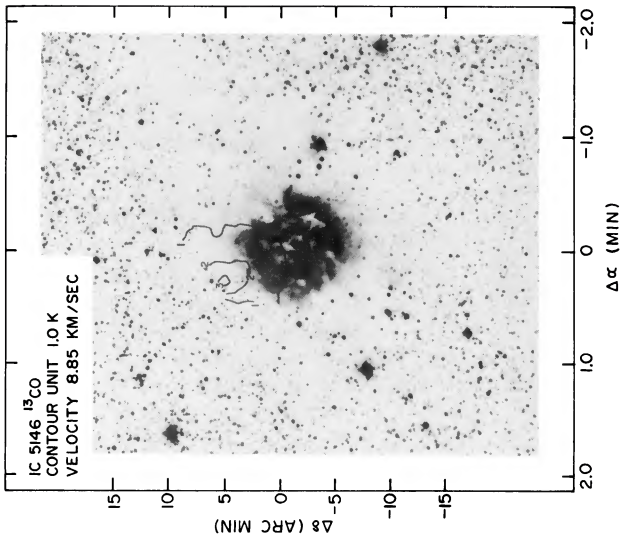

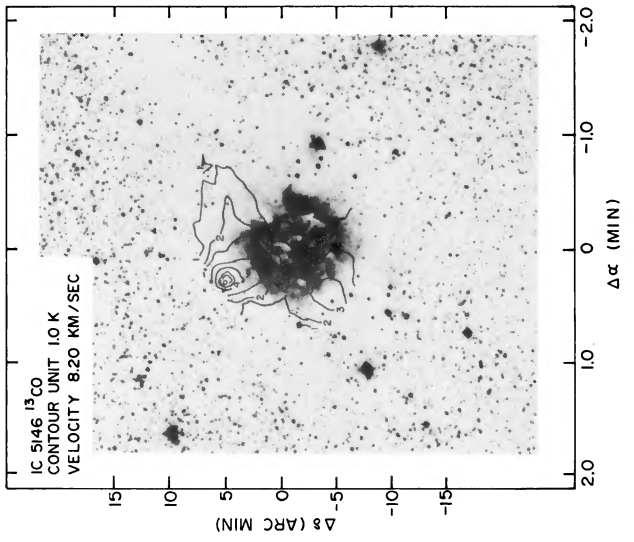

FIG. 5

FIGS. 4 and 5.—^{12}CO and ^{13}CO contours at different velocities placed on a photograph reproduced from the Palomar Sky Survey prints. The velocity interval corresponds to the resolution of the filters. Center coordinate is the same as in Fig. 1.

© American Astronomical Society • Provided by the NASA Astrophysics Data System

1982ApJ...256..139M

The change was small because of the offsetting variations in the partition function, optical depth, and the exponential term containing T_x.

The values for the masses of each concentration are listed in Table 1. The total mass of the three concentrations is 430 $M_\odot$ which is somewhat lower than that given by Lada and Elmegreen (1979). Each of the masses in Table 1 is significantly larger than that of the H II region which is 10 $M_\odot$ (Roger and Irwin 1982). If HS1 and HS2 are taken to be spherical in shape, the average density $n_{H_2} \approx 2500$–3000 cm^{-3}. If emission out to the lowest contour surrounding the H II region is included (see Fig. 1), the total mass of molecular gas could be increased to about 1000 $M_\odot$ (Israel 1980).

The energies of the clouds were calculated and are listed in Table 2 in the columns labeled $2T$ and V, which represent twice the internal kinetic energy and the potential energy, respectively. The kinetic energy term $2T = 3M\sigma_{v_r}$, where σ_{v_r} is the dispersion in radial velocity of the cloud profiles, and the potential energy is given by $\frac{3}{5}(GM^2/R)$. The values of these quantities for each cloud are similar, which indicates that the clouds are stable if the line broadening is caused by turbulent and thermal velocities. However, if the line broadening is a result of large-scale streaming motions, then the clouds are most likely collapsing (although expansion cannot be ruled out from the observations).

b) *Related Observations*

The $J = 2$–1 line of CS at 97.98 GHz, the existence of which indicates regions of higher density, was detected at peak 1 but not at peaks 4 or 6 using the same equipment as for CO. The line is quite weak, with an antenna temperature referred to outside the atmosphere of 0.5 K. The 3 σ upper limits for T_a at the other positions are 0.2 K. The molecular hydrogen densities implied by the detection of CS are $\sim 4 \times 10^4$ cm^{-3} (Turner *et al.* 1973), about 15 times that for CO. However, the weak lines imply a column density about an order of magnitude lower than the typical value of $\sim 10^{14}$ cm^{-2} (Turner *et al.* 1973; Gardner and Whiteoak 1978), indicating that the CS emission probably originates in a small core. This small core of higher density has negligible effect on the mass estimate above.

In an attempt to obtain further observational evidence relating to the nature of the three temperature-enhanced regions, we searched several positions, listed in Table 3, for 22 GHz H_2O maser emission. The 3 σ upper limit to any emission is 1.6 Jy. Negative results, although somewhat less sensitive and at different positions and epochs, were also obtained by Blitz and Lada (1978) and Lada and Elmegreen (1979).

TABLE 2

KINETIC AND POTENTIAL ENERGIES OF THE THREE HOT SPOTS

Hot Spot	Avg. Radius (pc)	$2T$ (10^{45} ergs)	V (10^{45} ergs)
1	0.65	3.7	4.8
2	0.41	1.1	1.1
3	0.71	0.8	0.6

TABLE 3

POSITIONS SEARCHED FOR H_2O EMISSION

α(1950)	δ(1950)	Comment
21^{h}51^{m}37^s	47°02′07″	
21 51 59	46 58 22	peak 1
21 52 06	46 59 37	
21 52 06	46 57 07	
21 51 52	47 07 07	peak 3
21 51 08	46 59 37	peak 6

There are no continuum sources associated with HS1 in the maps of Israel (1977) or of Roger and Irwin (1982) down to a level of about 7 mJy. Joyce (1978) has mapped at 3.5 μm a 3′.5 × 3′.5 grid centered on peak 1 using the Kitt Peak National Observatory (KPNO) 1.3 m telescope and sets a 3 σ upper limit of 90 mJy to any detection. Very recent observations by Sargent *et al.* (1981) at 85 and 150 μm (brought to our attention by a referee) strongly suggest an embedded source of luminosity $\sim 3 \times 10^3$ $L_\odot$ coincident with HS1. In the next section we consider the source of heating required to explain the CO emission.

c) *Internal Heating*

In the absence of a continuous heating source, HS1 would cool very quickly. Various authors have discussed the cooling of molecular clouds (see Goldsmith and Langer 1978). For the densities and temperatures encountered in this study (e.g., HS1 has $n_{H_2} \sim 4 \times 10^4$ cm^{-3}, and $T_k \sim 40$ K), ^{12}CO is the dominant coolant, and quantitatively similar results for this cooling have been obtained by Scoville and Solomon (1974), de Jong, Chu, and Dalgarno (1975), and Goldsmith and Langer (1978). Following Goldsmith and Langer, for $n_{H_2} = 10^4$ cm^{-3}, the total cooling rate as a function of temperature is given by

$$\frac{dE}{dt} = 1.5 \times 10^{-26} T^{2.7} \text{ ergs cm}^{-3} \text{ s}^{-1} . \quad (1)$$

Since the energy per unit volume of the gas, E, is also a function of temperature, a characteristic time scale for cooling is given by the expression

$$\tau_{cool} = 1.86 \times 10^{18} n_{H_2} k [T_f^{-1.7} - T_i^{-1.7}] \text{ yr} , \quad (2)$$

and for $n_{H_2} = 10^4$ cm^{-3}, $T_i = 40$ K, and $T_f = 20$ K, $\tau_{cool} \sim 10^4$ yr. This is a very short time scale, about 1% of the free-fall collapse time and about 10% of the estimated time since the H II region began expanding into the denser cloud (see § IV).

Various external heating mechanisms, such as cosmic-ray ionization, gravitational contraction, shocks, time dependent H_2 formation, and magnetic ion-neutral slip, have been discussed by Goldreich and Kwan (1974), Lada and Black (1976), Scalo (1977), Hill and Hollenbach (1978), Elmegreen, Dickinson, and Lada (1978), Goldsmith and Langer (1978), and Nachman (1979). Cosmic-

© American Astronomical Society • Provided by the NASA Astrophysics Data System

1982ApJ...256..139M

ray. heating by the excess energy from ionization is generally believed to be capable of maintaining clouds at temperatures which are in the range of 10–15 K. Thus HS1 clearly stands out as a source which has either recently formed or else has continuous heat input.

Because of the high degree of symmetry of HS1 and the lack of anomalous velocity structure, such as unusually wide lines or high velocities, the heating would, however, appear to be due to an embedded source. The concept of a protostar being responsible for the heating of a molecular cloud has been treated theoretically by Goldreich and Kwan (1974), Mezger, Smith, and Churchwell (1974), and Scoville and Kwan (1976). A thick circumstellar dust shell surrounding a pre–main-sequence star is opaque to wavelengths short of the infrared. The dust is then heated by infrared emission, and energy transfer between the dust and gas occurs through collisions. In radiative equilibrium, the dust temperature T_d depends upon the distance from the star r(pc) and luminosity L(ergs s^{-1}) as:

$$T_d = 22.9\left(\frac{L}{r^2 \times 10^{38}}\right)^{1/5} . \quad (3)$$

The constant outside the brackets is from Mezger, Smith, and Churchwell (1974) and is consistent with that derived by Scoville and Kwan (1976), who chose their values to model the Kleinmann-Low Nebula. This formula assumes a λ^{-1} emissivity dependence, one which has received some observational support (Gatley *et al.* 1977; Thronson and Harper 1979). The degree of coupling between the gas temperature T_{CO}, (the ^{12}CO kinetic temperature) and the dust temperature T_d is dependent on the density n_{H_2} (as may be seen by comparing the rate of cooling given by eq. [1] with the rate of heating given by Spitzer 1949). For reasons suggested by Scoville and Kwan (1976), it is expected that T_{CO} will be closely coupled to T_d even in clouds of moderate density ($n_{H_2} \sim 10^4$ cm^{-3}). Knapp *et al.* (1977) reached a similar conclusion. Observational evidence for this is presented by Thronson, Loewenstein, and Stokes (1979).

Using equation (3) and assuming $T_d = T_{CO}$, we find that the change in T_d, as a function of radius, for a star in the spectral range between B0.5 and B1 agrees well with the observed data for HS1, as shown in Figure 6. Luminosities were taken from Panagia (1973), and the observed data were taken along the northwest and southwest radial directions so that we are dealing with peak 1 only.

Thus an embedded protostellar source of spectral type close to B1 is the most plausible explanation for the existence of HS1. Indeed, Sargent *et al.* (1981) report far-infrared observations of IC 5146 and strongly suggest that an embedded source is present near the peak of HS1, thus substantiating our conjecture. Their reported value for T_d is 39 K, in good agreement with our CO maximum temperature, but their luminosity is lower than our predicted value by about a factor of 2. If the value of Sargent *et al.* is correct, then this must mean that there is some external heating due to the central star, BD +46°3474.

Sargent *et al.* also conclude that the other CO hot spots, HS2 and HS3, are most likely due to external heating from BD +46°3474.

As a final point, we note that the H I contours of Figure 2 show that H I emission is generally strong where CO emission is weak. This is expected, since H_2 would be readily dissociated by radiation from a B0 V star. Although there are regions where strong H I and CO

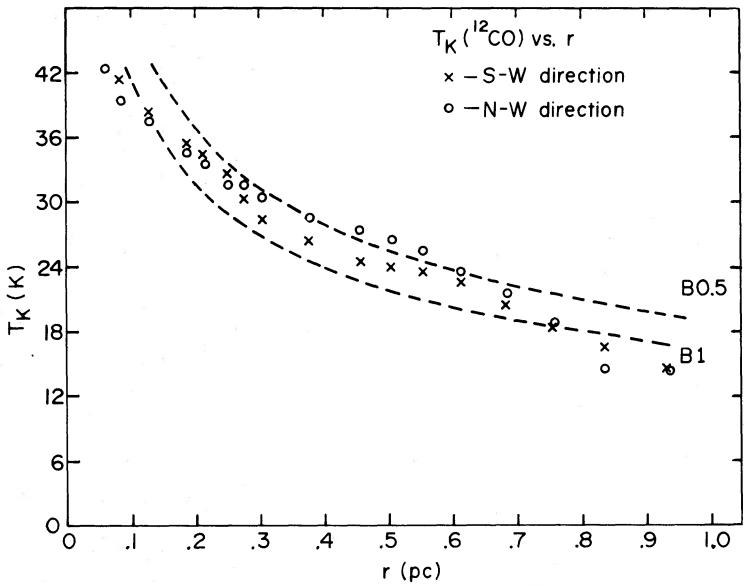

FIG. 6.—Kinetic temperature, obtained from ^{12}CO, as a function of radial distance in two directions from the center of the most intense region, HS1. The expected change in temperature as a function of radius for the dust heated by B0.5 and B1 stars is also shown.

© American Astronomical Society • Provided by the NASA Astrophysics Data System

1982ApJ...256..139M

emission coincide, such as HS1, there is probably not spatial coincidence in these cases. The total mass of the H I cloud associated with IC 5146 is 440 $M_\odot$, about the same as the total mass of the three molecular concentrations. The H I structure is elaborated further by Roger and Irwin (1982).

IV. VELOCITY STRUCTURE

Figure 7 shows CO LSR velocities obtained at positions along the extended lane to the northwest of S125. As previously reported (McCutcheon, Roger, and Dickman 1979; Israel 1980), these vary smoothly over a distance of 16.1 pc from S125 with a gradient of 0.26 km s^{-1} pc^{-1}, whereas the velocities (taken from Milman *et al.* 1975) over approximately the next 10.7 pc are constant. Velocity structure such as this would be difficult to explain if the extended lane were a single entity extending over 26.8 pc. However, Figure 1 indicates that the connection between the two dust lane segments having different velocity gradients is very weak (i.e., the dust lane is constricted at $\Delta\alpha \sim -6.0$ min), and perhaps the two sections are indeed unconnected. If this is the case, it is fortuitous that the velocities of the two segments are equal at the position where the velocity gradient changes, although velocity values of about +3 km s^{-1} are typical of spectral lines observed in discrete objects near this region (Ho, Martin, and Barrett 1978; Hjalmarson *et al.* 1977).

On the assumption that the 16.1 pc segment with the velocity gradient is a distinct dynamical structure, it is interesting to investigate its rotational stability using the virial theorem. In this case, $2T = 3M\sigma_{v_r}{}^2 + \frac{2}{3}M(\Delta V)^2$, where the second term is the rotational kinetic energy of the segment considered to be a long cylindrical rod rotating about one end, and ΔV is the velocity separation between the ends. From the data, $2T = 10.9 \times 10^6 M$ joules and, using $R = 16.1$ pc, $V = 8.1 \times 10^{-29} M^2$ joules. The mass is calculated, as before, from $N_{^{13}CO}$ which has an average value of 3×10^{15} cm^{-2}, which implies $N_{H_2} = 1.5 \times 10^{21}$ cm^{-2} (Dickman 1978).

If we assume the depth of the arm to be the same as its width (10′ or 2.6 pc) over a length of 61′ (or 16.1 pc), the mass is 1156 $M_\odot$. (Using the data from Milman *et al.* [1975], Lada and Elmegreen [1979] quote a value of 1950 $M_\odot$ for the mass out to 26 pc. Our value for this length is 1945 $M_\odot$, almost in exact agreement.)

If we include the hot spot masses from Table 1, the total mass for the segment being treated here as one entity is 1597 $M_\odot$. With this value, $2T = 42V$. (If the 16.1 pc segment were considered to be rotating about the middle, $2T = 14V$.) Thus, the mass does not appear to be nearly enough to make this extended arm stable and, indeed, the rotation is perhaps responsible for its elongated geometry. Another explanation would then be required for the other segment which shows constant velocities. However, it may have evolved differently and perhaps has associated magnetic fields. A study of another extended region, the L204 complex (McCutcheon, Vrba, and Dickman 1982), has revealed no rotation over an angular length of about 2°. However, this region appears to be associated with a magnetic field which has controlled its evolution and produced its elongated geometry. Samson (1976) has found the magnetic field in the immediate vicinity of S125 to be quite random, but no information is available regarding any field associated with the extended segment. Infrared

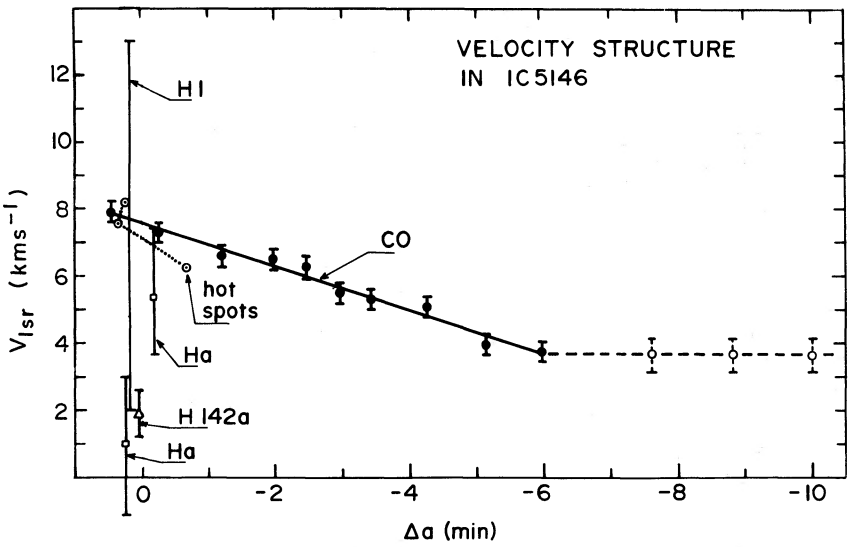

FIG. 7.—Velocity structure in the vicinity of IC 5146. Filled circles represent CO velocities from the present work. Open circles represent CO velocities obtained by Milman *et al.* (1975). The hot spot velocities are from the present work; the dotted line indicates the change in velocity between pairs. The H I velocity range is taken from Roger and Irwin (1982). The H142α velocity is from Kuiper, Knapp, and Rodriguez Kuiper (1976). Hα velocities are averages of individual velocities taken from Williamson (1970).

© American Astronomical Society • Provided by the NASA Astrophysics Data System

1982ApJ...256..139M

polarimetry measurements of background stars could be useful in establishing if there is a magnetic field and hence the significance of the rotation.

Other features of the gas, the molecular hot spot velocities, and the range of H I velocities (Roger and Irwin 1982) are shown on the velocity plot of Figure 7 along with features of the H II region, the variation in Hα velocities (Williamson 1970), and the H142α velocity (Kuiper, Knapp, and Rodriguez Kuiper 1976). The three hot spots occur at different velocities, as determined from Figures 4 and 5, and indicate a more complicated structure than the cooler, less dense background gas, i.e., there is a N–S velocity gradient as well as an E–W one. This may be just the result of random velocities in the gas from which the dense clouds were formed. The H I velocities cover a fairly large range and in general do not show the fine structure (i.e., over a velocity range of 1–2 km s^{-1}) seen in the molecular clouds because of the much larger line widths of 7–8 km s^{-1}. However, contour maps at velocities differing by $\sim$6 km s^{-1} do show structure (Roger and Irwin 1982) with the H I at the largest velocities lying on the far side of the H II region. This structure is still evident in Figure 2 where the H I contours shown have been integrated over the same velocity range as CO. The inner contour of H I is in the form of a ring around the H II region. The H I at larger velocities ($\sim$8.5–12 km s^{-1}) does not show this ringlike structure.

An interesting feature of Figure 7 is the large difference between the H142α velocity, which is the average velocity of the H II region as a whole, and the background gas. Considering this relative velocity to be a result of the expansion of the H II region, we can apply the classical expansion theory to estimate an age. The radius of an H II region, as a function of time, is given by Spitzer (1978):

$$r_s = r_{so}\left(1 + \frac{7}{4}\frac{C_{II}\,t}{r_{so}}\right)^{4/7} \equiv r_{so}x^{4/7}\,, \qquad (4a)$$

and the velocity of expansion is then:

$$v_s = C_{II}\,x^{-3/7}\,, \qquad (4b)$$

where $C_{II} = 10$ km s^{-1} is the velocity of sound in the H II region, and r_{so} is the initial equilibrium Strömgren radius. For a B0 star $r_{so}(n_H{}^2)^{1/3} = 22$ (Spitzer 1978). Since the values of $N_{^{13}CO}$ in the vicinity of S125 are influenced by the presence of the H II region, we use $n_H = 200$ (Roger and Irwin 1982). Hence $r_{so} = 0.64$ pc. From either equation (4a) or (4b), the value of the age t to give the observed radius $r_s = 1.4$ pc and the observed velocity difference $v_s = 5.6$ km s^{-1} is 1.0×10^5 yr. However, since S125 is on the near side of the dark cloud and the expansion on the far side of the H II region would encounter a much higher density than on the side facing the observer, an age calculated from a nonuniform density model would be more appropriate. (See, e.g., the Champagne models of Tenorio-Tagle [1979], Bodenheimer, Tenorio-Tagle, and Yorke [1979], Tenorio-Tagle, Yorke, and Bodenheimer [1979], which indicate that the expansion age will be smaller than that given by the above calculation.) The derived age for a nonuniform density model of IC 5146 is 9.4×10^4 yr (Roger and Irwin 1982). This is a factor of 30 lower than the age given for the cluster by Walker (1959).

Figure 7 also shows Hα velocities from Williamson (1970). The two values are averages of values from the west and east sides of the nebula at the central declination for our observations and, although the errors involved are rather large (the values quoted on individual points are as large as 6 km s^{-1}), there is a difference in the average velocities of the lines from the two sides. This may indicate a more complicated motion for the ionized gas than assumed above (perhaps a braking of the west side as suggested by Williamson) and that perhaps v_s may be somewhat different. Nevertheless, because of the uncertainties involved we have ignored these values and have determined v_s from the more precise H142α velocity (which, because of the beamwidth, is an average over most of the nebula).

V. SUMMARY AND CONCLUSION

The IC 5146 region is unique, with a nearly circular H II region, S125, the presence of a large H I cloud, and the geometry of an elongated arm to the west. One of the major components of the region is the molecular gas which is studied here.

$J = 1$–0 CO observations in the vicinity of IC 5146 have revealed several interesting features. Three separate regions of enhanced emission were detected around the periphery of S125, and the masses of these regions, along with the various emission peaks detected, are listed in Table 1. The overall structure is similar to that detected by Lada and Elmegreen (1979), but our positions and masses differ somewhat. The most intense region, denoted HS1, requires an internal heat source, particularly if its age is similar to that of the H II region. Our observations are consistent with the heat source being an embedded pre–main-sequence star with a luminosity close to that of a B1 star; a conclusion confirmed by Sargent *et al.* (1981). Figure 2 shows that H I emission is generally strong where CO emission is weak. This would be expected since H I is formed from dissociated H_2.

There is interesting velocity structure in the immediate vicinity of S125 and along the extended arm, as shown in Figure 7. The arm shows a velocity gradient of 0.26 km s^{-1} pc^{-1} out to a distance of 16.1 pc. Calculations using the virial theorem show that in the absence of magnetic fields the cloud cannot be stable if it is rotating. Rotation may be the reason for its elongated geometry. The next cloud segment, out to 26.8 pc, has no measurable velocity gradient, although it is not clear whether the two segments are physically connected. The hot spot peaks occur at distinct velocities, and the gradients between them are not the same as that measured for the extended dust lane. The H II region has a much smaller mass (10 $M_\odot$) than any of the three enhanced regions, and its expansion is not likely to be influencing the kinematics of these regions. Rather, the velocities of the

© American Astronomical Society • Provided by the NASA Astrophysics Data System

1982ApJ...256..139M

hot spots may reflect random motions that existed before their formation. Alternatively, these velocities may be the result of turbulence caused by the formation of S125.

S125 has a velocity, as determined from the H142α line, distinctly different from the background molecular gas, and from this, using classical expansion theory, we estimate an age of approximately 10^5 yr. This is a factor of 30 less than the age given for the cluster.

The evolution of H II regions has been described in a general way by Mathews and O'Dell (1969) and in more detail by the Champagne models of Tenorio-Tagle (1979), Bodenheimer, Tenorio-Tagle, and Yorke (1979), and Tenorio-Tagle, Yorke, and Bodenheimer (1979). After the formation of the initial Strömgren sphere, the expansion of the H II region has undoubtedly heated and compressed the molecular gas, leading to the formation of the three regions of enhanced emission. Subsequent star formation is most likely occurring in the hottest of these regions, HS1.

We are grateful to Dr. R. Joyce who kindly provided the near-infrared upper limit. We thank the referee for drawing our attention to the unpublished infrared observations of Sargent *et al.* (1981). W. H. M. gratefully acknowledges grants in aid of research from the Natural Sciences and Engineering Research Council of Canada. R. L. D.'s research was partly supported by the Aerospace Corporation's Programs for Research and Investigation.

REFERENCES

Blair, G. N., Evans, N. J., II, Vanden Bout, P. A., and Peters, W. L., III. 1978, *Ap. J.*, **219**, 896.
Blitz, L., and Lada, C. J. 1978, *Ap. J.*, **227**, 152.
Bodenheimer, P., Tenorio-Tagle, G., and Yorke, H. W. 1979, *Ap. J.*, **233**, 85.
de Jong, T., Chu, Shih-I, and Dalgarno, A. 1975, *Ap. J.*, **199**, 69.
Dickman, R. L. 1978, *Ap. J. Suppl.*, **37**, 407.
Dickman, R. L., McCutcheon, W. H., and Shuter, W. L. H. 1979, *Ap. J.*, **234**, 100.
Elias, J. H. 1978, *Ap. J.*, **223**, 859.
Elmegreen, B. G., Dickinson, D. F., and Lada, C. J. 1978, *Ap. J.*, **220**, 853.
Evans, N. J., II, Blair, G. N., and Beckwith, S. 1977, *Ap. J.*, **217**, 448.
Field, G. B. 1973, in *Molecules in the Galactic Environment*, ed. M. A. Gordon and L. E. Snyder (New York: Wiley), p. 42.
Gardner, F. F., and Whiteoak, J. B. 1978, *M.N.R.A.S.*, **183**, 711.
Gatley, I., Becklin, E. E., Werner, M. E., and Wynn-Williams, C. G. 1977, *Ap. J.*, **216**, 277.
Goldreich, P., and Kwan, J. 1974, *Ap. J.*, **189**, 441.
Goldsmith, P. F., and Langer, W. D. 1978, *Ap. J.*, **222**, 881.
Hill, J. K., and Hollenbach, D. J. 1978, *Ap. J.*, **225**, 390.
Hjalmarson, Å., Sume, A., Elldér, J., Rydbeck, O. E. H., Moore, E. L., Huguenin, G. R., Sandqvist, A., Lindblad, P. O., and Lindroos, P. 1977, *Ap. J. Suppl.*, **35**, 263.
Ho, P. T. P., Martin, R. N., and Barrett, A. H. 1978, *Ap. J.* (*Letters*), **221**, L117.
Israel, F. P. 1977, *Astr. Ap.*, **60**, 233.
———. 1978, *Astr. Ap.*, **70**, 769.
———. 1980, *A.J.*, **85**, 1612.
Joyce, R. 1978, private communication.
Knapp, G. R., Kuiper, T. B. H., Knapp, S. L., and Brown, R. L. 1977, *Ap. J.*, **214**, 78.
Kuiper, T. B. H., Knapp, G. R., and Rodriguez Kuiper, E. N. 1976, *Astr. Ap.*, **48**, 475.
Lada, C. J., and Black, J. H. 1976, *Ap. J.* (*Letters*), **203**, L75.
Lada, C. J., and Elmegreen, B. G. 1979, *A.J.*, **84**, 336.
Mathews, W. G., and O'Dell, C. R. 1969, *Ann. Rev. Astr. Ap.*, **7**, 67.
McCutcheon, W. H., Dickman, R. L., Shuter, W. L. H., and Roger, R. S. 1980, *Ap. J.*, **237**, 9.
McCutcheon, W. H., Roger, R. S., and Dickman, R. L. 1979, *Bull. AAS*, **11**, 714.
McCutcheon, W. H., Vrba, F. J., and Dickman, R. L. 1982, in preparation.
Mezger, P. G., Smith, L. F., and Churchwell, E. 1974, *Astr. Ap.*, **32**, 269.
Milman, A. S., Knapp, G. R., Knapp, S. L., and Wilson, W. J. 1975, *A.J.*, **80**, 101.
Nachman, P. 1979, *Ap. J. Suppl.*, **39**, 103.
Panagia, N. 1973, *A.J.*, **78**, 929.
Riegel, K. W. 1967, *Ap. J.*, **148**, 87.
Roger, R. S., and Irwin, J. A. 1982, *Ap. J.*, **256**, 127.
Samson, W. B. 1976, *Ap. Space Sci.*, **44**, 217.
Sargent, A. I., van Duinen, R. J., Fridlund, C. V. M., Nordh, H. L., and Aalders, J. W. G. 1981, preprint.
Scalo, J. M. 1977, *Ap. J.*, **213**, 705.
Scoville, N. Z., and Kwan, J. 1976, *Ap. J.*, **206**, 718.
Scoville, N. Z., and Solomon, P. M. 1974, *Ap. J.* (*Letters*), **187**, L67.
Spitzer, L. 1949, *Ap. J.*, **109**, 337.
———. 1978, *Physical Processes in the Interstellar Medium* (New York: Wiley).
Tenorio-Tagle, G. 1979, *Astr. Ap.*, **71**, 59.
Tenorio-Tagle, G., Yorke, H. W., and Bodenheimer, P. 1979, *Astr. Ap.*, **80**, 110.
Thronson, H. A., Jr., and Harper, D. A. 1979, *Ap. J.*, **230**, 133.
Thronson, H. A., Jr., Loewenstein, R. F., and Stokes, G. M. 1979, *A.J.*, **84**, 1328.
Turner, B. E., Zuckerman, B., Palmer, D., and Morris, M. 1973, *Ap. J.*, **186**, 123.
Walker, M. F. 1959, *Ap. J.*, **130**, 57.
Williamson, R. A. 1970, *Ap. Space Sci.*, **6**, 45.

R. L. DICKMAN: Five College Radio Observatory, University of Massachusetts, Amherst, MA 01003

W. H. McCUTCHEON: Department of Physics, University of British Columbia, Vancouver, B.C. V6T 1W5, Canada

R. S. ROGER: Dominion Radio Astrophysical Observatory, Herzberg Institute of Astrophysics, P.O. Box 248, Penticton, B.C. V2A 6K3, Canada

© American Astronomical Society • Provided by the NASA Astrophysics Data System